



# HHS Public Access

Author manuscript

Nat Commun. Author manuscript; available in PMC 2015 March 23.

Published in final edited form as:

Nat Commun. ; 5: 4989. doi:10.1038/ncomms5989.

## Rapid *in vivo* detection of isoniazid-sensitive *Mycobacterium tuberculosis* by breath test

Seong Won Choi<sup>#2</sup>, Mamoudou Maiga<sup>#3</sup>, Mariama C. Maiga<sup>3</sup>, Viorel Atudorei<sup>4</sup>, Zachary D. Sharp<sup>4</sup>, William R. Bishai<sup>3</sup>, and Graham S. Timmins<sup>2</sup>

<sup>2</sup> Dept. Pharmaceutical Sciences, College of Pharmacy, University of New Mexico, Albuquerque NM 87131 USA.

<sup>3</sup> Center for Tuberculosis Research, Department of Medicine, Johns Hopkins University, Baltimore MD 21231 USA.

<sup>4</sup> Dept. Earth and Planetary Sciences, College of Pharmacy, University of New Mexico, Albuquerque NM 87131 USA

# These authors contributed equally to this work.

### Abstract

There is urgent need for rapid, point of care diagnostic tools for tuberculosis (TB) and drug sensitivity. Current methods based on *in vitro* growth take weeks, while DNA amplification can neither differentiate live from dead organisms nor determine phenotypic drug resistance. Here we show the development and evaluation of a rapid breath test for isoniazid (INH)-sensitive TB based on detection of labeled N<sub>2</sub> gas formed specifically from labeled INH by mycobacterial KatG enzyme. *In vitro* data shows the assay is specific, dependent on mycobacterial abundance, and discriminates between INH-sensitive and resistant (S315T mutant KatG) TB. *In vivo*, the assay is rapid with maximal detection of <sup>15</sup>N<sub>2</sub> in exhaled breath of infected rabbits within five to ten minutes. No increase in <sup>15</sup>N<sub>2</sub> is detected in un-infected animals, and the increases in <sup>15</sup>N<sub>2</sub> are dependent on infection dose. This test may allow rapid detection of INH-sensitive TB.

### Introduction

Bacterially-activated prodrugs are unusually well-represented among the first- and second-line TB drugs. These include not only established drugs such as isoniazid <sup>1</sup>, ethionamide <sup>2</sup> or

Users may view, print, copy, and download text and data-mine the content in such documents, for the purposes of academic research, subject always to the full Conditions of use:[http://www.nature.com/authors/editorial\\_policies/license.html#terms](http://www.nature.com/authors/editorial_policies/license.html#terms)

Corresponding author: GST (gtimmins@salud.unm.edu).

#### Author Contributions

SC developed techniques, performed *in vitro* bacteriology and isotope ratio experiments, analyzed IRMS data, and wrote manuscript. MM developed techniques, performed *in vivo* experiment, analyzed data and wrote manuscript. MCM performed *in vivo* experiments and analyzed data. VA developed techniques, performed and analyzed IRMS analysis. ZDS developed techniques, performed and analyzed IRMS analysis and wrote manuscript. WRB designed experiments, analyzed *in vivo* data, and wrote manuscript. GST synthesized chemicals, designed experiments, analyzed *in vivo* data, and wrote manuscript.

#### Conflict of Interest Statement

GST acts as Chief Science Officer of, and WRB consults for, Avisa Pharma, a company that is developing a clinical-stage <sup>13</sup>C urea-based stable isotope breath test for detection of TB and other urease producing lung infections. The rest of the authors declare no conflicts of interest.

pyrazinamide<sup>3</sup>, but also newly approved and developing agents such as the nitroimidazoles delamanid<sup>4</sup> and PA-824<sup>5</sup>. The selectivity of these agents arises from their specific activation by mycobacterial enzymes, usually to reactive intermediates, and is underlined by the major mode of resistance to these agents being mutations in genes of their activating enzymes such as *katG* for INH<sup>6</sup>, *ethA* for ethionamide<sup>7</sup>, *pncA* for pyrazinamide<sup>8</sup> and *ddn* for nitroimidazoles<sup>9</sup>. Since gene inactivation may occur through a multiplicity of single nucleotide polymorphisms (SNPs) or insertion/deletion (indel) events, nucleic acid amplification and SNP-indel detection approaches provide only partially predictive drug susceptibility data. Beyond single gene mutational resistance, multiple other alleles<sup>10-14</sup> and other drugs<sup>15,16</sup> may influence enzymatic activity of prodrug conversion, factors that may also limit nucleic acid based techniques for drug susceptibility testing. Despite the importance of prodrug activation, studies have been limited to *in vitro* samples or bacterial culture, and at present there are no POC techniques to directly measure prodrug conversion and enzymatic activity.

The mycobacterial enzyme KatG, which is responsible for INH activation, produces a range of INH-derived radicals that react with cellular components, especially the isonicotinoyl acyl radical (INAcyl) that adds covalently to NAD<sup>+</sup> and NADP<sup>+</sup>. The adducts formed by these radicals are potent inhibitors of key mycobacterial targets. The first target of such inhibition to be elucidated was 2-trans-enoyl-acyl carrier protein reductase (InhA) which binds INAcyl-NAD<sup>+</sup> adducts tightly inhibiting mycolic acid synthesis<sup>17</sup>. Although other targets or reactive species may play roles, the importance of these alternative mechanisms compared to the widely accepted inhibition of InhA remains unclear<sup>18</sup>.

The detection of degradation products of the INAcyl-NAD<sup>+</sup> adduct, such as 4-isonicotinoylnicotinamide (4-INN) in urine or other fluids held great promise as a measure of INH prodrug conversion in TB, and so determining KatG activity<sup>19</sup>. However, this appears to lack specificity for *M. tuberculosis* as 4-INN was found in urine of uninfected mice treated with INH, and in urine of TB patients even when they were culture-negative after treatment<sup>19</sup>.

Mycobacterial KatG activates INH by oxidation to a hydrazyl radical that undergoes beta scission to form INAcyl radical. The other product of this beta-scission reaction, diazene, has received little to no attention in the literature. To study diazene production in KatG expressing mycobacteria, we used doubly <sup>15</sup>N<sub>2</sub>-hydrazyl labeled INH (1) to produce doubly labeled diazene (Fig. 1A). Under physiologic conditions this diazene rapidly undergoes either oxidation by unsaturated bonds (Figure 1b)<sup>20</sup> or bimolecular disproportionation (Figure 1c) to produce <sup>15</sup>N<sub>2</sub><sup>21</sup>. Diazene is widely used synthetically in the stereospecific reduction of a wide range of carbon-carbon double bonds<sup>22</sup>.

This <sup>15</sup>N<sub>2</sub> produced from INH-derived diazene may be readily detected by isotope ratio mass spectrometry (IRMS), and its abundance is reported as δ<sup>15</sup>N<sub>2</sub> where δ<sup>15</sup>N<sub>2</sub> = 1000 x [(<sup>15</sup>N<sup>15</sup>N/<sup>14</sup>N<sup>14</sup>N)<sub>Sample</sub> - (<sup>15</sup>N<sup>15</sup>N/<sup>14</sup>N<sup>14</sup>N)<sub>Standard</sub>]/(<sup>15</sup>N<sup>15</sup>N/<sup>14</sup>N<sup>14</sup>N)<sub>Standard</sub>

Atmospheric <sup>15</sup>N is much lower in abundance than <sup>14</sup>N (~ 0.36%), hence <sup>15</sup>N<sub>2</sub> is very low in abundance (~ 13 ppm) so even small amounts of <sup>15</sup>N<sub>2</sub> generation may be detected through

changes in  $\delta^{15}\text{N}_2$ . For example, an increase in the value of  $\delta^{15}\text{N}_2$  of 250 would indicate a 25% increase in the absolute amount of  $^{15}\text{N}_2$  in a sample. This same principle is exploited by other isotope ratio breath diagnostics including the urease breath test for of *Helicobacter pylori* infection.

In this report, we describe the detection of  $^{15}\text{N}_2$  products of INH activation that are specific for mycobacterial KatG, and test their specificity against other important lung bacterial pathogens that possess related peroxidase enzymes. By measuring the increase over baseline  $\delta^{15}\text{N}_2$  upon addition of the  $^{15}\text{N}_2$ -hydrazyl INH (a method termed INH $\rightarrow$ N here), we hypothesized that IRMS detection of this  $^{15}\text{N}_2$  may allow sensitive measurement of INH activation by KatG.

## Results

*In vitro* cultures of *Mycobacterium tuberculosis* H37Rv or *Mycobacterium bovis* BCG were treated with  $^{15}\text{N}_2$ -hydrazyl INH in sealed tubes and portions of headspace gas collected, filtered and analyzed. Treatment with 1 mg/ml  $^{15}\text{N}_2$ -hydrazyl INH resulted in marked increases in  $\delta^{15}\text{N}_2$  which were dependent upon bacterial density (CFU/ml) (Fig. 2A). Next we determined the correlation between the accumulated  $\delta^{15}\text{N}_2$  and the dose of  $^{15}\text{N}_2$ -hydrazyl INH administered (Fig. 2B), and these experiments showed sensitive IRMS detection of headspace  $\delta^{15}\text{N}_2$  following  $^{15}\text{N}_2$ -hydrazyl INH doses of 0.1 mg/ml, a concentration we subsequently used throughout. The generation of headspace  $\delta^{15}\text{N}_2$  occurred rapidly (Fig. 2C), and plateau levels were reached in approximately one hour. Similar data were also observed with *M. bovis* BCG (Fig. 3) another KatG-expressing mycobacterial species, although generally lower levels of  $^{15}\text{N}_2$  production were observed compared to *M. tuberculosis* H37Rv. These data confirmed our ability to measure of mycobacterial KatG activity quantitatively by IRMS monitoring of conversion of  $^{15}\text{N}_2$ -hydrazyl INH to  $^{15}\text{N}_2$  using *in vitro* cultures of mycobacteria.

We then evaluated the specificity of our  $^{15}\text{N}_2$ -hydrazyl INH to  $^{15}\text{N}_2$  detection method for mycobacterial KatG activity. As may be seen in Fig. 4A the common respiratory pathogens *S. aureus*, *P. aeruginosa* and *E. coli* did not produce  $^{15}\text{N}_2$  when treated with  $^{15}\text{N}_2$ -hydrazyl INH. To determine whether our  $^{15}\text{N}_2$ -hydrazyl INH to  $^{15}\text{N}_2$  detection method for INH prodrug conversion was specific for the mycobacterial KatG, we tested the production of  $^{15}\text{N}_2$  using an *M. tuberculosis* strain harboring a mutated KatG. This strain possessed the *M. tuberculosis katG-S315T* mutation that is known to profoundly decrease INH activation and result in drug resistance.<sup>6</sup> When compared to *M. tuberculosis* H37Rv, we found the *katG-S315T* mutant did not produce any measurable  $^{15}\text{N}_2$  (Fig. 4B).

These *in vitro* characteristics supported our hypothesis that the  $^{15}\text{N}_2$ -hydrazyl INH to  $^{15}\text{N}_2$ , INH $\rightarrow$ N detection method might be used to detect KatG activation of INH *in vivo*, using a breath test approach<sup>23,24</sup>. Rabbits were infected with high dose ( $10^4$  CFU) or low dose ( $10^3$  CFU) *M. tuberculosis* H37Rv using an inhalation exposure system (Glas-col) as previously described<sup>25</sup>. After a six week incubation period, rabbits were treated with 10 mg of  $^{15}\text{N}_2$ -hydrazyl INH instilled bronchoscopically. Direct delivery to the lung was chosen to rapidly expose lung bacteria to  $^{15}\text{N}_2$ -hydrazyl INH in order to allow rapid assay, as opposed to an

oral dosage form which would require absorption and redistribution. Inhaled INH has been used clinically in humans.<sup>26</sup> Breath samples were collected prior to dosing, and then at 5, 10 and 20 minutes post-dose. Four non-infected rabbits were used as control group.

It was seen that  $\delta^{15}\text{N}_2$  increased rapidly in breath of all infected animals, with no observed increase in breath  $\delta^{15}\text{N}_2$  of the four uninfected controls (Fig. 5A, 5B). The lack of signal in uninfected animals, together with significant signals in all infected animals, suggests that a high degree of sensitivity and specificity is inherent in this assay. Breath  $\delta^{15}\text{N}_2$  reached a maximum after 5 to 10 minutes, and then variably decreased, likely due to differential distribution and absorption of  $^{15}\text{N}_2$ -hydrazyl INH from the lung into systemic circulation from the more focal pattern of delivery arising from instillation. A relationship between peak levels of  $\delta^{15}\text{N}_2$  and lung CFU was observed (Fig. 6A and 6B reflecting  $\delta^{15}\text{N}_2$  as a function of lung CFU at sacrifice and initial infective CFU respectively). This suggests the approach might be sensitive to the amount of lung mycobacteria present, although significant further work is needed to delineate this relationship. Repetitive use of the technique is also likely to be complicated by the highly bactericidal nature of inhaled INH, and for monitoring of bacterial load other techniques such as urease breath tests<sup>23</sup> or sputum CFU may be more useful.

## Discussion

The INH $\rightarrow$ N detection method for mycobacterial KatG activity described here is capable of discriminating between INH susceptible and resistant *M. tuberculosis* and between KatG-expressing mycobacteria and other common lung pathogens *in vitro*. It is also capable of rapidly discriminating between controls and animals infected with INH-susceptible TB. Potential advantages of the INH $\rightarrow$ N test are the rapid non-radioactive breath test approach, based upon detecting prodrug activation, and that samples the entire lung. The readout of this test,  $^{15}\text{N}_2$ , is detected using IRMS, and portable MS detection devices are available and under development<sup>29</sup> supporting eventual development into a POC technology. Residual gas analyzer MS, a technique with great potential for portability, has recently been shown effective in clinical IRMS<sup>30</sup>, and represents one avenue forwards. As with any new potential diagnostic approach, ultimate clinical usage and utility must be determined in trials.

Clinically, high-level INH resistance is strongly correlated to *katG*-S315T mutations with greatly lowered INH activating (and INH $\rightarrow$ N) activity, whereas lower level resistance is associated with *inhA* promoter mutations that will likely not be differentiated from INH sensitive strains by the INH $\rightarrow$ N test<sup>31</sup>. However, INH $\rightarrow$ N assay would allow rapid point of care detection of *katG*-S315T and other *katG* mutations as part of a diagnostic approach, to enable rapid and optimal therapy. The potential for the INH $\rightarrow$ N method to report as a rapid and specific biomarker of mycobacterial load may provide useful tool for monitoring clinical trials and therapeutic efficacy. INH $\rightarrow$ N may also prove useful in diagnosis of some non-tuberculous mycobacteria, such as INH-sensitive *M. kansasii*,<sup>32</sup> that can otherwise be challenging. However, since some peroxidases other than mycobacterial KatG enzymes bind INH (such as lactoperoxidase<sup>33</sup>) further studies of specificity are planned.

Similar approaches may also be extended to other TB prodrug classes so that effective and rapid detection of drug sensitivity/resistance through prodrug conversion can guide therapy. One example would be Delamanid and PA824 that are activated to bactericidal NO $\cdot$  by mycobacterial Ddn<sup>5</sup>: using <sup>15</sup>N-nitro-PA824 would result in <sup>15</sup>NO $\cdot$  that could be directly detected in breath, or as <sup>15</sup>N-nitrate/nitrite in other samples such as blood or urine. This could provide rapid detection of drug activation (and hence sensitivity) in patients when conventional techniques such as MS detection of des-nitro-PA824 are difficult (Clif Barry, personal communication). This would allow optimal use of these drugs in therapy of multi-drug resistant (MDR) and extensively-drug resistant (XDR) disease.

More generally, while pathogen genotypes are rapidly determined without culture, the study of bacterial phenotypes in the host (as opposed to culture in which it can greatly change) is extremely challenging. However, the broad importance of phenotype and phenotype variance in pathogenesis is becoming increasingly appreciated, with specific examples of both growth phase-dependent<sup>34</sup> and stochastic<sup>35</sup> isoniazid resistant phenotypes being recently elucidated. The ability to determine bacterial phenotypes through stable isotope detection of specific bacterial metabolic pathways without requiring culture could prove broadly valuable in complementing genomic approaches in studying microbiomes. Finally, it is worth noting that yet another reactive species from mycobacterial KatG activation of INH, in this case diazene, could play a role in INH action through reducing key unsaturated mycobacterial molecules.

## Methods

### Bacterial cultures

**Mycobacterium tuberculosis**—H37Rv (H37Rv), *M. bovis* BCG, *E. coli* DH5 $\alpha$  and *P. aeruginosa* PAO1 were gifts from Professor Vojo Deretic,<sup>37,38</sup> *M. tuberculosis katGS315T* (*katG*-S315T) was a gift from Professor Alex Pym<sup>36</sup>. *S. aureus* USA300 LAC was a gift from Professor Pamela Hall<sup>39</sup>. All bacterial cultures were grown at 37°C with shaking. Mycobacterium cultures were prepared by thawing frozen stock aliquots: H37Rv and *katG*-S315T were grown in 7H9 Middlebrook liquid medium supplemented with oleic acid, albumin, dextrose and catalase (Becton Dickinson, Inc., Sparks, MD), 0.5% glycerol and 0.05% Tween 80. BCG was grown in the same culture medium omitting oleic acid. *Escherichia coli* DH5 $\alpha$  was grown overnight in LB broth (Becton Dickinson), *Pseudomonas aeruginosa* strain PAO1 was grown overnight in LB broth supplemented with 1.76% NaCl and 1% glycerol, and *Staphylococcus aureus* USA300 LAC was grown overnight in BBL Trypticase soybroth (Becton Dickinson).

### In vitro KatG assay

3 ml of mycobacterial cultures (BCG, H37Rv or *katG*-S315T) were diluted as appropriate from week-old cultures, while other bacterial cultures (*P. aeruginosa*, *E. coli* or *S. aureus*) were diluted from overnight cultures. The 3 ml cultures were shaken aerobically and then were incubated with <sup>15</sup>N<sub>2</sub>-hydrazyl INH (at 0.1 mg/ml unless noted) in 12 ml Exetainer vials (Labco Ltd., Ceredigion, UK) for 1 hour at 37 with shaking at 250 rpm unless otherwise

indicated. Collected headspace gas (1 ml) was filtered through 0.25 micron syringe filters and transferred into Helium-flushed Exetainers.

### Measurement of $^{15}\text{N}_2$ conversion

Sampled gas was analyzed for  $^{15}\text{N}$  enrichment in headspace  $\text{N}_2$  by gas isotope ratio mass spectrometry (Delta<sup>plus</sup>XL, Thermo Scientific Inc. Waltham, MA). Samples were separated by GC immediately upstream of their inlet into the IRMS using a 30 m column packed with 5 Å molecular sieves operating at 60°C and using ultra high purity helium as carrier gas. IRMS of the  $\text{N}_2$  peak measured relative ratio of mass 30  $^{15}\text{N}_2$  vs. mass 28  $^{14}\text{N}_2$ . Nitrogen gas of purity >99.99% (Matheson Tri-Gas, Albuquerque, NM) was used as reference gas.

### Animal experiments

These consisted of four uninfected control rabbits, two rabbits infected at high dose (N3 and N4) and two rabbits infected at low dose (N5 and N6). Rabbits (females, 16-20 weeks old, 3.5 - 4 Kg pathogen-free outbred New Zealand White, Robinson Services, Inc., Mocksville, NC) were aerosol infected with *M. tuberculosis* H37Rv at either  $10^3$  or  $10^4$  CFUs using an inhalation exposure system as previously described<sup>40</sup> (Glas-col, Terre Haut, IN). At week 6, rabbits were anesthetized with ketamine 15-25 mg/kg and xylazine 5-10 mg/kg, and then 10 mg  $^{15}\text{N}_2$ -hydrazyl-INH in 0.4 ml saline was instilled using intra-tracheal insertion through an endotracheal tube. To collect breath gas, a 14-French feeding tube connected to a 30 ml syringe was introduced through the endotracheal tube into the level of the carina to aspirate the exhaled air when rabbit is breathing out. Breath gas (12 ml) was filtered with a 0.35-micron filter into Helium-flushed tubes before and after  $^{15}\text{N}_2$ -hydrazyl-INH treatment at 0, 5, 10, and 20 min.  $^{15}\text{N}_2$  enrichment in breath gas was measured by IRMS. Immediately after breath testing, the animals were euthanized, and lung weight and CFU measured (Table 1). Rabbits were euthanized with intravenous euthasol (Virbac Corporation, Fort Worth, TX). The rabbit model was chosen as it is the smallest model that enables ready endoscopic infection, instillation of INH, and collection of breath.

### Ethics statement

Animal work in this study was carried out in strict accordance with the recommendations in the Guide for the Care and Use of Laboratory Animals of the National Institutes of Health, the Animal Welfare Act and US federal law. The protocol was approved by the Institutional Animal Care and Use Committees at Johns Hopkins University (RB11M466).

### Statistical analysis

All statistical analyses were performed using SPSS version 19 (SPSS Inc., Chicago, IL). *P* values were determined using ANOVA and Students' *t*-test, and values <0.05 considered statistically significant.

### Acknowledgements

Funded by NIH Grants AI064386 and AI081015 (GST) and AI36973 and AI37856 (WRB).



## References

1. Zhang Y, Heym B, Allen B, Young D, Cole S. The catalase-peroxidase gene and isoniazid resistance of *Mycobacterium tuberculosis*. *Nature*. 1992; 358:591–593. [PubMed: 1501713]
2. Baulard AR, et al. Activation of the pro-drug ethionamide is regulated in mycobacteria. *The Journal of biological chemistry*. 2000; 275:28326–28331. doi:10.1074/jbc.M003744200. [PubMed: 10869356]
3. Zhang Y, Mitchison D. The curious characteristics of pyrazinamide: a review. *The international journal of tuberculosis and lung disease : the official journal of the International Union against Tuberculosis and Lung Disease*. 2003; 7:6–21.
4. Matsumoto M, et al. OPC-67683, a nitro-dihydro-imidazooxazole derivative with promising action against tuberculosis in vitro and in mice. *PLoS medicine*. 2006; 3:e466. doi:10.1371/journal.pmed.0030466. [PubMed: 17132069]
5. Singh R, et al. PA-824 kills nonreplicating *Mycobacterium tuberculosis* by intracellular NO release. *Science*. 2008; 322:1392–1395. doi:10.1126/science.1164571. [PubMed: 19039139]
6. Heym B, Alzari PM, Honore N, Cole ST. Missense mutations in the catalase-peroxidase gene, *katG*, are associated with isoniazid resistance in *Mycobacterium tuberculosis*. *Molecular microbiology*. 1995; 15:235–245. [PubMed: 7746145]
7. Morlock GP, Metchock B, Sikes D, Crawford JT, Cooksey RC. *ethA*, *inhA*, and *katG* loci of ethionamide-resistant clinical *Mycobacterium tuberculosis* isolates. *Antimicrobial agents and chemotherapy*. 2003; 47:3799–3805. [PubMed: 14638486]
8. Scorpio A, Zhang Y. Mutations in *pncA*, a gene encoding pyrazinamidase/nicotinamidase, cause resistance to the antituberculous drug pyrazinamide in *tubercle bacillus*. *Nature medicine*. 1996; 2:662–667.
9. Manjunatha UH, et al. Identification of a nitroimidazo-oxazine-specific protein involved in PA-824 resistance in *Mycobacterium tuberculosis*. *Proceedings of the National Academy of Sciences of the United States of America*. 2006; 103:431–436. doi:10.1073/pnas.0508392103. [PubMed: 16387854]
10. Zahrt TC, Song J, Siple J, Deretic V. Mycobacterial *FurA* is a negative regulator of catalase-peroxidase gene *katG*. *Mol Microbiol*. 2001; 39:1174–1185. [PubMed: 11251835]
11. Pagan-Ramos E, Song J, McFalone M, Mudd MH, Deretic V. Oxidative stress response and characterization of the *oxyR-ahpC* and *furA-katG* loci in *Mycobacterium marinum*. *J Bacteriol*. 1998; 180:4856–4864. [PubMed: 9733688]
12. Lucarelli D, Vasil ML, Meyer-Klaucke W, Pohl E. The Metal-Dependent Regulators *FurA* and *FurB* from *Mycobacterium tuberculosis*. *International journal of molecular sciences*. 2008; 9:1548–1560. doi:10.3390/ijms9081548. [PubMed: 19169435]
13. Master S, Zahrt TC, Song J, Deretic V. Mapping of *Mycobacterium tuberculosis katG* promoters and their differential expression in infected macrophages. *J Bacteriol*. 2001; 183:4033–4039. [PubMed: 11395468]
14. Wakamoto Y, et al. Dynamic persistence of antibiotic-stressed mycobacteria. *Science*. 2013; 339:91–95. doi:10.1126/science.1229858. [PubMed: 23288538]
15. Flipo M, et al. Ethionamide boosters. 2. Combining bioisosteric replacement and structure-based drug design to solve pharmacokinetic issues in a series of potent 1,2,4-oxadiazole *EthR* inhibitors. *Journal of medicinal chemistry*. 2012; 55:68–83. doi:10.1021/jm200825u. [PubMed: 22098589]
16. Frenois F, Engohang-Ndong J, Loch C, Baulard AR, Villeret V. Structure of *EthR* in a ligand bound conformation reveals therapeutic perspectives against tuberculosis. *Molecular cell*. 2004; 16:301–307. doi:10.1016/j.molcel.2004.09.020. [PubMed: 15494316]
17. Rozwarski D, Grant G, Barton D, Jacobs W, Sacchettini J. Modification of the NADH of the isoniazid target (*InhA*) from *Mycobacterium tuberculosis*. *SCIENCE*. 1998; 279:98–102. [PubMed: 9417034]
18. Wang F, et al. *Mycobacterium tuberculosis* dihydrofolate reductase is not a target relevant to the antitubercular activity of isoniazid. *Antimicrobial agents and chemotherapy*. 2010; 54:3776–3782. doi:10.1128/AAC.00453-10. [PubMed: 20566771]

19. Mahapatra S, et al. A novel metabolite of antituberculosis therapy demonstrates host activation of isoniazid and formation of the isoniazid-NAD<sup>+</sup> adduct. *Antimicrobial agents and chemotherapy*. 2012; 56:28–35. doi:10.1128/AAC.05486-11. [PubMed: 22037847]
20. Tang HR, Mckee ML, Stanbury DM. Absolute Rate Constants in the Concerted Reduction of Olefins by Diazene. *J Am Chem Soc*. 1995; 117:8967–8973. doi:10.1021/Ja00140a011.
21. Tang HR, Stanbury DM. Direct-Detection of Aqueous Diazene - Its Uv Spectrum and Concerted Dismutation. *Inorg Chem*. 1994; 33:1388–1391. doi:10.1021/Ic00085a029.
22. Pasto DJ, Taylor RT. Reduction with diimide. *Organic Reactions*. 1991
23. Jassal MS, et al. 13[C]-urea breath test as a novel point-of-care biomarker for tuberculosis treatment and diagnosis. *Plos One*. 2010; 5:e12451. doi:10.1371/journal.pone.0012451. [PubMed: 20805989]
24. Maiga M, et al. In vitro and in vivo studies of a rapid and selective breath test for tuberculosis based upon mycobacterial CO dehydrogenase. *mBio*. 2014; 5:e00990. doi:10.1128/mBio.00990-14. [PubMed: 24736224]
25. Be NA, Klinkenberg LG, Bishai WR, Karakousis PC, Jain SK. Strain-dependent CNS dissemination in guinea pigs after Mycobacterium tuberculosis aerosol challenge. *Tuberculosis*. 2011; 91:386–389. doi:10.1016/j.tube.2011.07.003. [PubMed: 21831713]
26. Yokota S, Miki K. [Effects of INH (Isoniazid) inhalation in patients with endobronchial tuberculosis (EBTB)]. *Kekkaku : [Tuberculosis]*. 1999; 74:873–877.
27. Barry CE, et al. The spectrum of latent tuberculosis: rethinking the biology and intervention strategies. *Nature Reviews Microbiology*. 2009; 7:845–855. [PubMed: 19855401]
28. Pai M. Spectrum of latent tuberculosis—existing tests cannot resolve the underlying phenotypes. *Nature Reviews Microbiology*. 2010; 8:242–242.
29. Ouyang Z, Noll RJ, Cooks RG. Handheld miniature ion trap mass spectrometers. *Analytical chemistry*. 2009; 81:2421–2425. doi:10.1021/ac900292w. [PubMed: 19281190]
30. Maity A, et al. Residual gas analyzer mass spectrometry for human breath analysis: a new tool for the non-invasive diagnosis of Helicobacter pylori infection. *J Breath Res*. 2014; 8:016005. [PubMed: 24566134]
31. Dantes R, et al. Impact of isoniazid resistance-conferring mutations on the clinical presentation of isoniazid monoresistant tuberculosis. *PloS one*. 2012; 7:e37956. doi:10.1371/journal.pone.0037956. [PubMed: 22649569]
32. Griffith DE, et al. An official ATS/IDSA statement: diagnosis, treatment, and prevention of nontuberculous mycobacterial diseases. *American journal of respiratory and critical care medicine*. 2007; 175:367–416. [PubMed: 17277290]
33. Singh AK, et al. Mode of binding of the tuberculosis prodrug isoniazid to heme peroxidases: binding studies and crystal structure of bovine lactoperoxidase with isoniazid at 2.7 Å resolution. *J Biol Chem*. 2010; 285:1569–1576. doi:10.1074/jbc.M109.060327. [PubMed: 19907057]
34. Niki M, et al. A novel mechanism of growth phase-dependent tolerance to isoniazid in mycobacteria. *Journal of Biological Chemistry*. 2012; 287:27743–27752. [PubMed: 22648414]
35. Wakamoto Y, et al. Dynamic persistence of antibiotic-stressed mycobacteria. *Science*. 2013; 339:91–95. [PubMed: 23288538]
36. Pym AS, Saint-Joanis B, Cole ST. Effect of katG mutations on the virulence of Mycobacterium tuberculosis and the implication for transmission in humans. *Infect Immun*. 2002; 70:4955–4960. [PubMed: 12183541]
37. Curcic R, Dhandayuthapani S, Deretic V. Gene expression in mycobacteria: transcriptional fusions based on xyle and analysis of the promoter region of the response regulator mtrA from Mycobacterium tuberculosis. *Mol Microbiol*. 1994; 13:1057–1064. [PubMed: 7854120]
38. Schurr MJ, Martin DW, Mudd MH, Deretic V. Gene cluster controlling conversion to alginate-overproducing phenotype in Pseudomonas aeruginosa: functional analysis in a heterologous host and role in the instability of mucoidy. *J Bacteriol*. 1994; 176:3375–3382. [PubMed: 8195094]
39. Hall PR, et al. Nox2 modification of LDL is essential for optimal apolipoprotein B-mediated control of agr type III Staphylococcus aureus quorum-sensing. *PLoS pathogens*. 2013; 9:e1003166. doi:10.1371/journal.ppat.1003166. [PubMed: 23459693]



40. Converse PJ, et al. The Impact of Mouse Passaging of Mycobacterium tuberculosis Strains prior to Virulence Testing in the Mouse and Guinea Pig Aerosol Models. *PloS one*. 2010; 5 doi:ARTN e10289 DOI 10.1371/journal.pone.0010289.
41. Li Z, Kelley C, Collins F, Rouse D, Morris S. Expression of katG in Mycobacterium tuberculosis is associated with its growth and persistence in mice and guinea pigs. *Journal of Infectious Diseases*. 1998; 177:1030–1035. [PubMed: 9534978]
42. Wilson TM, Lisle GW, Collins DM. Effect of inhA and katG on isoniazid resistance and virulence of Mycobacterium bovis. *Molecular microbiology*. 1995; 15:1009–1015. [PubMed: 7623658]

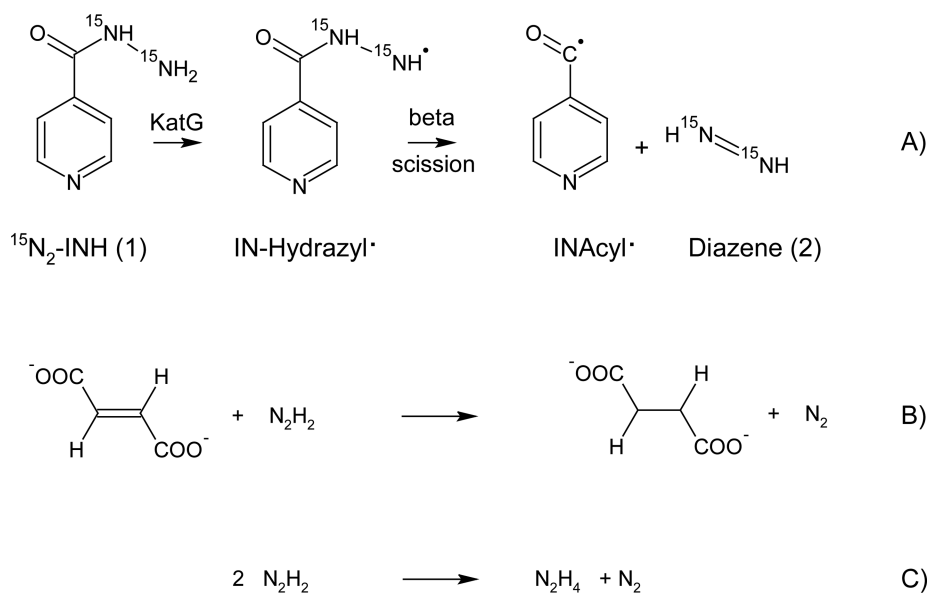


**Fig. 1. Production of  $\text{N}_2$  from KatG ctivation of Isoniazid**

(A) Production of labeled diazene from  $^{15}\text{N}_2$ -hydrazyl- INH; (B) oxidation of diazene to  $\text{N}_2$  by reaction with unsaturated carbon bonds such as fumarate shown, rate constant  $8 \times 10^2 \text{ M}^{-1} \text{ s}^{-1}$  <sup>20</sup>; (C) disproportionation of diazene to  $\text{N}_2$  and hydrazine rate constant  $2.2 \times 10^4 \text{ M}^{-1} \text{ s}^{-1}$  <sup>21</sup>.

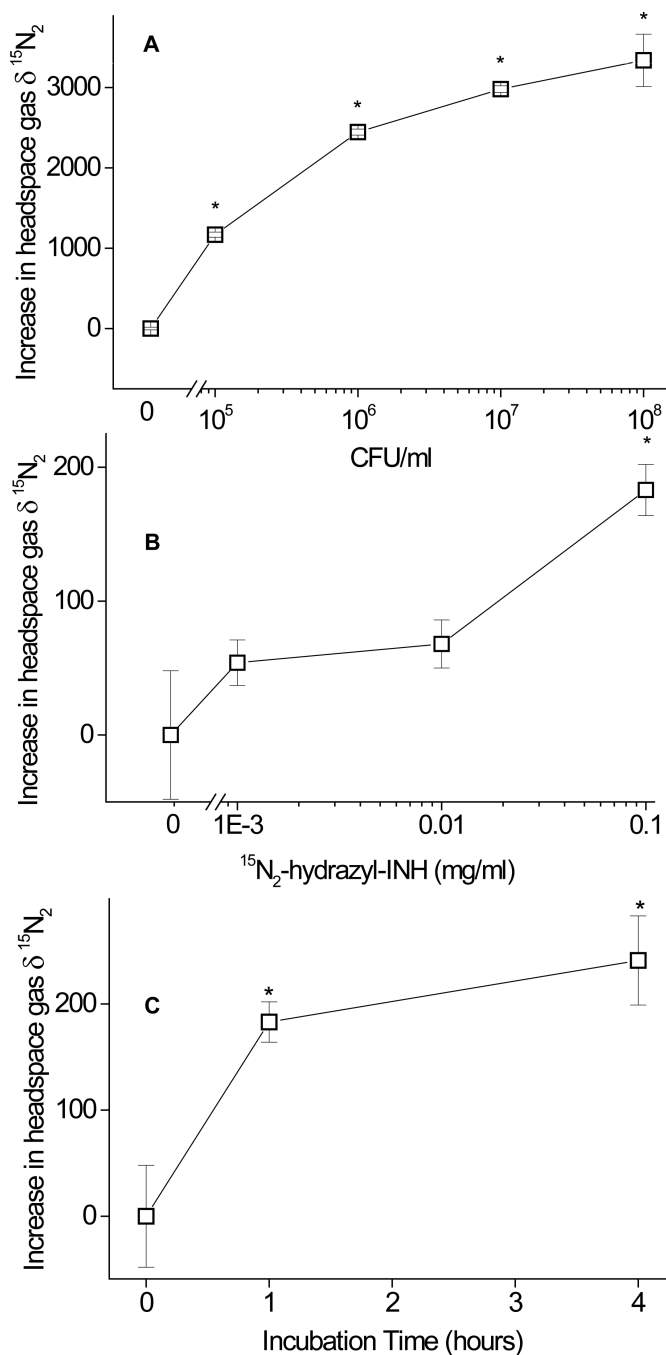


**Fig. 2. CFU, Dose and Time Dependence of  $^{15}\text{N}_2$  Production by *M. tuberculosis* H37Rv** Increased headspace  $\delta^{15}\text{N}_2$  (mass 30) in  $^{15}\text{N}_2$ -hydrazyl INH-treated cultures.  $^{15}\text{N}_2$  production was dependent upon: (A) bacterial density of *M. tuberculosis* H37Rv (3 ml) incubated with  $^{15}\text{N}_2$ -hydrazyl-INH (1 mg/ml) for 1 hour,  $*p < 0.001$ ; (B) concentration of  $^{15}\text{N}_2$ -hydrazyl INH (H37Rv ( $10^8$  CFU/ml, 3 ml) was incubated with  $^{15}\text{N}_2$ -hydrazyl-INH at the indicated dose for 1 hour,  $*p < 0.001$ ); (C) incubation time (H37Rv ( $10^8$  CFU/ml, 3 ml) was incubated with  $^{15}\text{N}_2$ -hydrazyl-INH (0.1 mg/ml) for the indicated time,  $*p < 0.001$ ). Data

represent mean  $\pm$  STD of 4 separate biological replicates. One-way ANOVA with Tukey *post hoc* test.

Author Manuscript

Author Manuscript

Author Manuscript

Author Manuscript

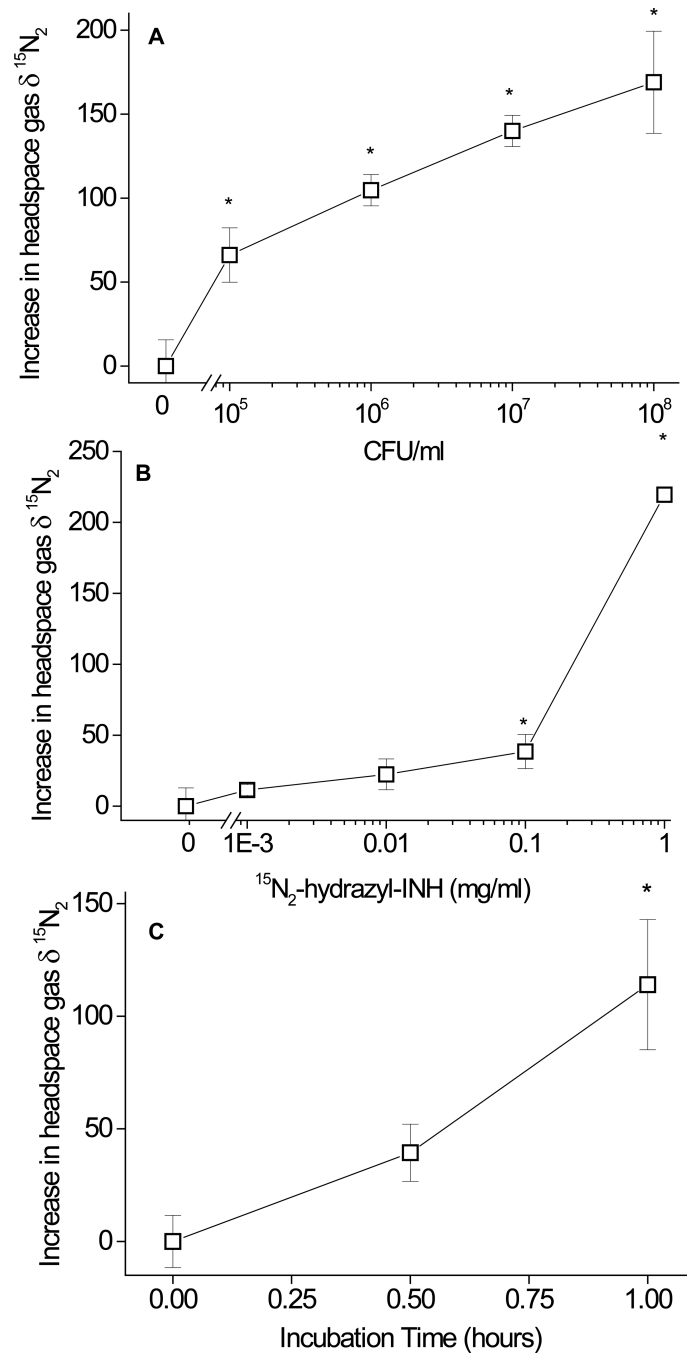


**Fig. 3. CFU, Dose and Time Dependence of  $^{15}\text{N}_2$  Production by *M. bovis* BCG**  
 Increased headspace  $\delta^{15}\text{N}_2$  (mass 30) in  $^{15}\text{N}_2$ -hydrazyl INH-treated cultures was dependent upon: (A) bacterial density of *M. bovis* BCG (3 ml) incubated with 1 mg/ml of  $^{15}\text{N}_2$ -hydrazyl-INH for 1 hour,  $*p < 0.001$ ; (B) concentration of  $^{15}\text{N}_2$ -hydrazyl INH (*M. bovis* BCG ( $10^8$  CFU/ml, 3 ml) was incubated with  $^{15}\text{N}_2$ -hydrazyl-INH at the indicated dose for 1 hour,  $*p < 0.001$ ); (C) incubation time (*M. bovis* BCG ( $10^8$  CFU/ml, 3 ml) was incubated with  $^{15}\text{N}_2$ -hydrazyl-INH (1 mg/ml) for the indicated time,  $*p < 0.001$ ). Data represent mean  $\pm$  STD of 3 separate biological replicates. One-way ANOVA with Tukey *post hoc* test.

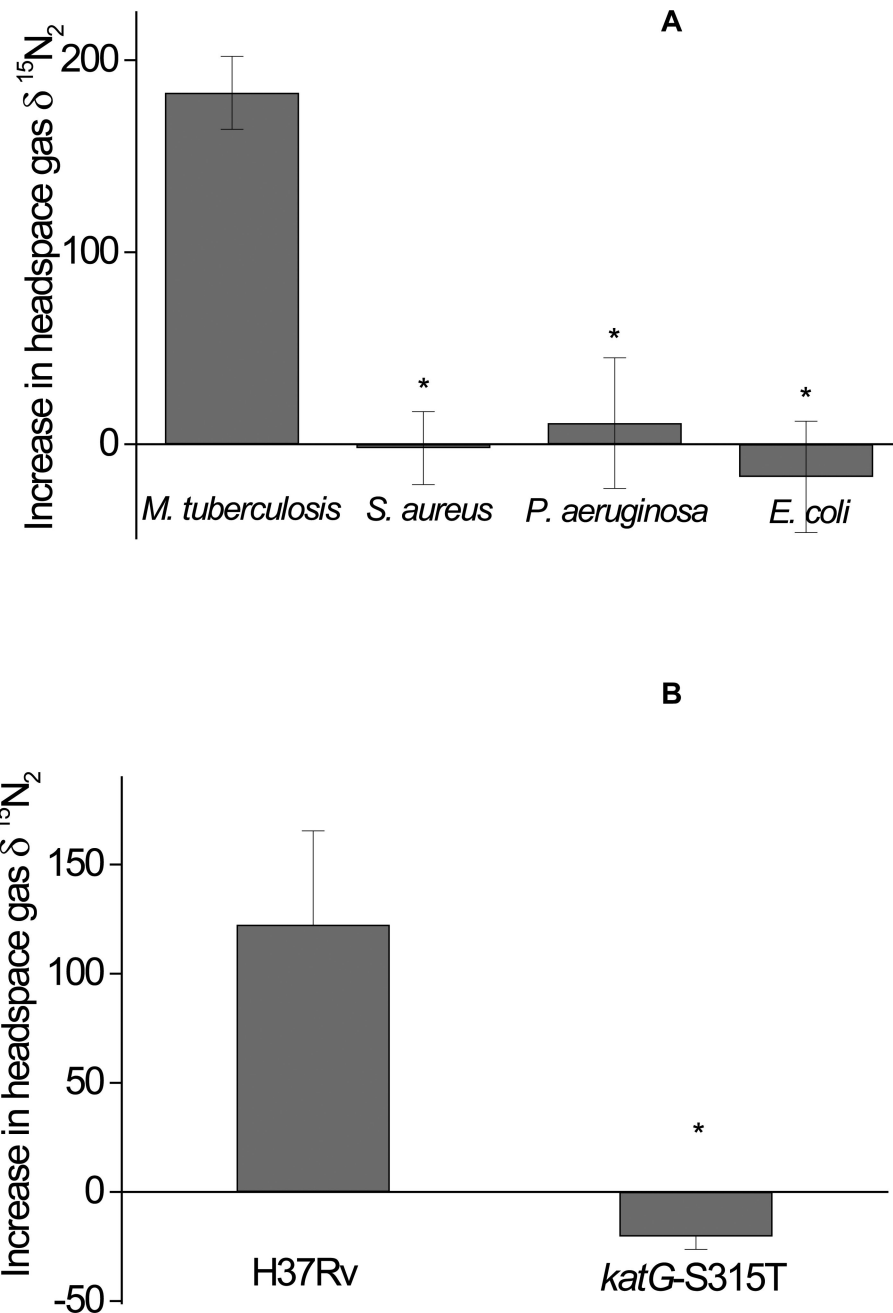


**Fig. 4. Specificity of  $^{15}\text{N}_2$  production**

(A) Increased headspace  $\delta^{15}\text{N}_2$  in  $^{15}\text{N}_2$ -hydrazyl INH treated overnight cultures of *S. aureus*, *P. aeruginosa* and *E. coli* compared to *M. tuberculosis* H37Rv. Bacterial culture ( $10^8$  CFU/ml, 3 ml) was incubated with  $^{15}\text{N}$ -INH (0.1 mg/ml) for 1 hour. Data represent mean  $\pm$  STD ( $n=3$  biological replicates). Students' *t*-test,  $*p<0.001$ . (B) Comparison in headspace  $\delta^{15}\text{N}_2$  in  $^{15}\text{N}_2$ -hydrazyl INH-treated drug-sensitive *M. tuberculosis* H37Rv, and an INH-resistant KatG mutant strain (*katG-S315T*). H37Rv or *katG-S315T* strains ( $10^8$  CFU/ml, 3 ml) were incubated with  $^{15}\text{N}_2$ -hydrazyl INH (0.1 mg/ml) for 1 hour. Data represent mean  $\pm$  STD ( $n=4$  biological replicates). Students' *t*-test,  $*p<0.005$ .



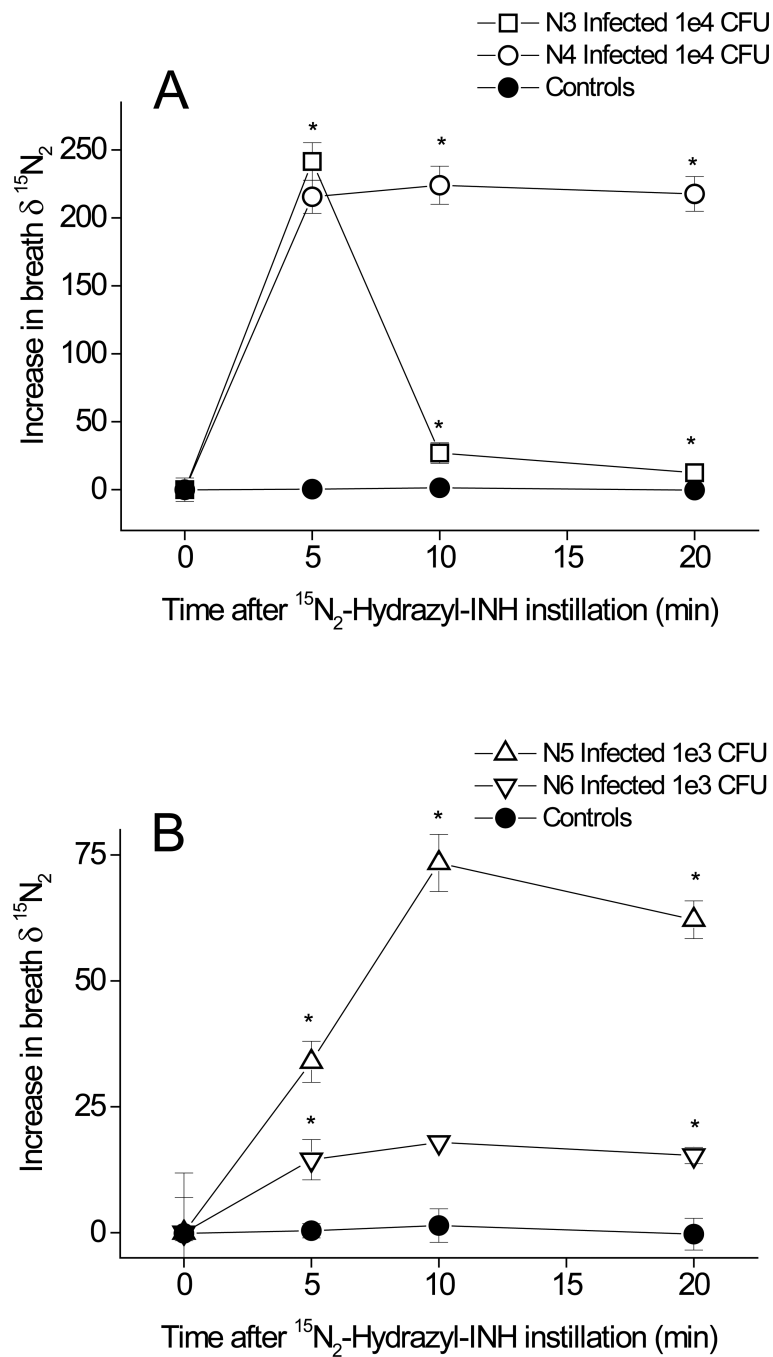


**Fig. 5. *In vivo*  $^{15}\text{N}_2$  Production in TB-Infected and Control rabbits**

Increased breath in (A) high dose, and (B) low dose TB infected rabbits. Rabbits were infected with high or low doses of *M. tuberculosis* H37Rv, instilled with 10 mg  $^{15}\text{N}_2$ -hydrazyl INH and breath collected. Rabbits (pathogen-free outbred New Zealand White) were infected with the indicated CFU by aerosol. At week 6, rabbits were anesthetized with ketamine (15-25 mg/kg) and xylazine (5-10 mg/kg), and treated with  $^{15}\text{N}_2$ -hydrazyl-INH (10 mg/ in 0.4 ml phosphate buffered saline) by intratracheal intubation. Exhaled breath gas (12 ml) was collected into Helium gas-flushed tubes at 0, 5, 10, and 20 min post  $^{15}\text{N}_2$ -

hydrazyl INH administration. Data represent mean  $\pm$  STD ( $n=3$  repeats for each rabbit N3 through N6,  $n=12$  for four uninfected control rabbits with 3 repeats for each). Two-way mixed ANOVA with Bonferroni *post hoc* test.  $*p<0.001$ . See detailed rabbit data in Table 1.

Author Manuscript

Author Manuscript

Author Manuscript

Author Manuscript

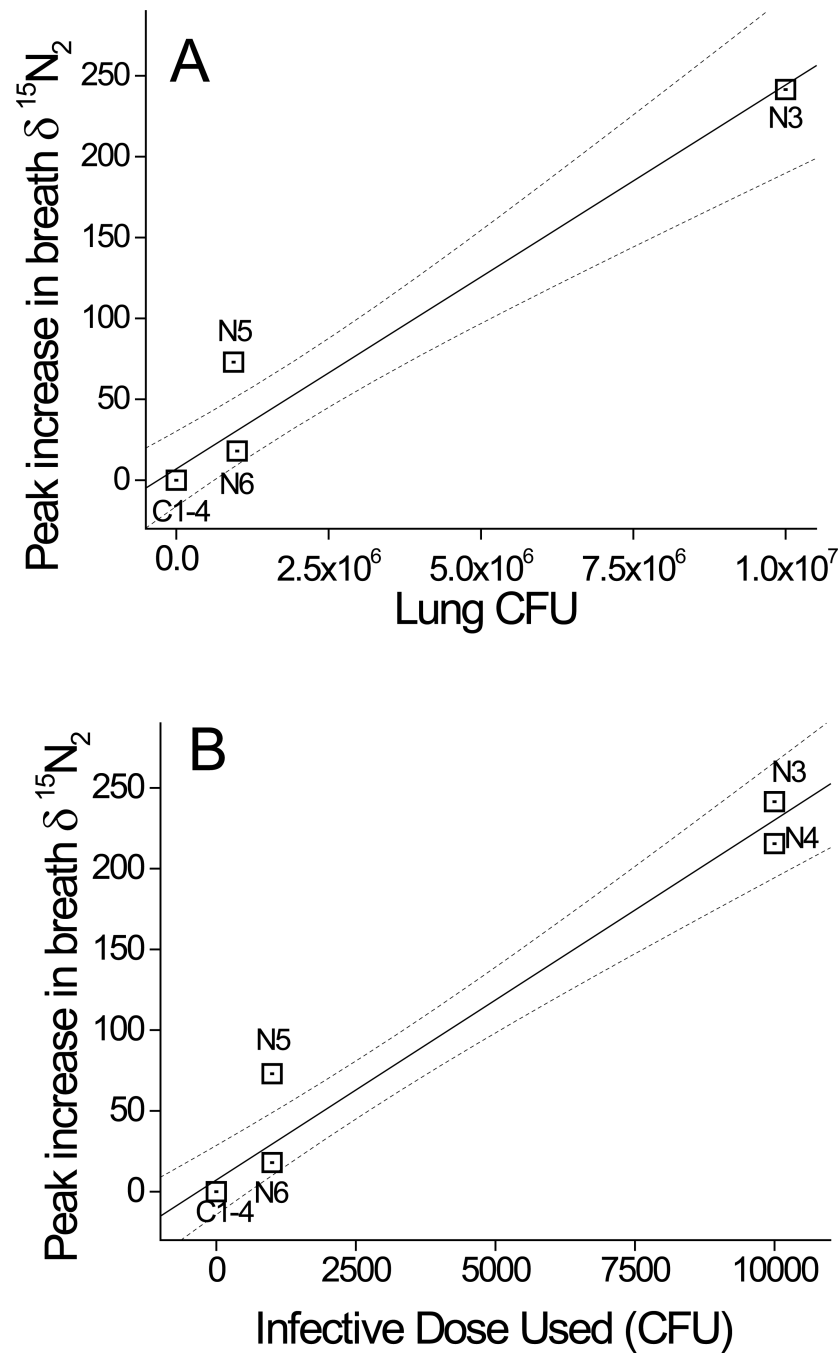


**Fig. 6. Dependence of peak increase in breath  $\delta^{15}\text{N}_2$  upon infection level**  
 The maximal increase in breath  $\delta^{15}\text{N}_2$  after  $^{15}\text{N}_2$ -hydrazyl INH delivery in Fig.5 is plotted here as a function of (A) lung CFU determined at sacrifice, and (B) initial infective dose delivered. Rabbit identity numbers are shown, and 95% confidence limits presented as dashed lines.

**Table 1**

Details of TB-infected rabbits.

| Rabbit ID#                | N3                    | N4                  | N5                    | N6                    |
|---------------------------|-----------------------|---------------------|-----------------------|-----------------------|
| Inoculum size             | 10 <sup>4</sup> CFU   | 10 <sup>4</sup> CFU | 10 <sup>3</sup> CFU   | 10 <sup>3</sup> CFU   |
| CFU / g lung at sacrifice | 1.8 × 10 <sup>5</sup> | ND                  | 7.6 × 10 <sup>4</sup> | 7.4 × 10 <sup>4</sup> |
| Lung weight (g)           | 58                    | ND                  | 12.5                  | 14.1                  |
| Total lung CFU            | 1 × 10 <sup>7</sup>   | ND                  | 9.4 × 10 <sup>5</sup> | 1 × 10 <sup>6</sup>   |

ND, not performed.

Author Manuscript

Author Manuscript

Author Manuscript

Author Manuscript